Degradation of Protein in Nanoplasma Generated around Gold Nanoparticles in Solution by Laser Irradiation

Yoshihiro Takeda*

East Tokyo Laboratory, Genesis Research Institute, Inc., 717-86 Futamata, Ichikawa, Chiba 272-0001, Japan

Tamotsu Kondow

Cluster Research Laboratory, Toyota Technological Institute, 717-86 Futamata, Ichikawa, Chiba 272-0001, Japan

Fumitaka Mafuné

Department of Basic Science, Graduate School of Arts and Sciences, The University of Tokyo, Komaba, Meguro-ku, Tokyo 153-8902, Japan

Received: July 11, 2005

We developed a method of protein degradation in an aqueous solution containing gold nanoparticles by irradiation of a pulse laser. In the present study, lysozyme was used as an example. Lysozyme degradation proceeded most efficiently when a pH of the solution was adjusted so that it was at the isoelectric point. The scheme of the lysozyme degradation is as follows: (1) Lysozyme molecules in the solution are neutralized and adsorbed on the gold nanoparticles with its pH value adjusted at the isoelectric point, (2) nanoplasma is generated in the close vicinity of a gold nanoparticle which is excited by an intense 532-nm laser, (3) lysozyme molecules in the nanoplasma are degraded into small fragments. Lysozyme degradation does not proceed efficiently at a pH value deviated from the isoelectric point because the lysozyme molecules are dissolved uniformly so that only a small portion of the lysozyme molecules are located in the vicinity of gold nanoparticles which create the nanoplasma.

1. Introduction

Plasma induced by irradiation by an intense laser in an aqueous solution has attracted much attention because it not only plays a key role in fundamental physical processes in laser−matter interactions,[1−8] but also has a vital utility in practical applications such as spectrochemical analysis of chemical species in aqueous media[9−13] and biomedical applications such as laser surgery.[14−16] Plasma initiated by laser irradiation is a stochastic event and is usually characterized by a threshold electron density, which is estimated to be as high as $\sim 10^{18}$ cm^{-3} in the focal volume.[17] This electron density can be attained by cascade ionization initiated by multiphoton ionization and pure multiphoton ionization. The cascade ionization occurs if a free seed-electron in the focal volume is accelerated by absorbing photons and liberates bound electrons by collision.[6−8] The liberated electrons are accelerated further by absorbing additional photons and liberate more electrons, forming electron avalanches leading to plasma.

Plasma is induced differently by laser irradiation on small particles (seed-electron sources) dispersed in an aqueous solution.[18,19] For instance, in an aqueous solution dispersed with gold nanoparticles, plasma is generated primarily by initiating cascade ionization on the gold nanoparticles. When a laser intense enough for the gold nanoparticles to undergo multiphoton ionization but not for water to do so is allowed to irradiate the solution, a free seed-electron ejected from a laser-excited gold nanoparticle creates plasma in the vicinity of the gold nanoparticle.

Plasma created around a laser-excited gold nanoparticle in an aqueous solution is confined within a volume of several tens of cubic nanometers and, hence, is named "nanoplasma", as described in the Discussion section. By taking advantage of the nanoplasma confinement, one can fabricate various methods of processing at a molecular scale. In the present report, we exemplified a vital utility of nanoplasma by demonstration of the efficient and selective degradation of a protein dissolved in an aqueous solution containing gold nanoparticles under the irradiation of a laser. Particularly, the degradation of lysozyme was investigated in this work. In this method, protein molecules are selectively adsorbed onto gold nanoparticles by adjusting the pH of the solution. By doing so, the adsorbed protein molecules are degraded most efficiently because nanoplasma is confined in the vicinity of photoexcited gold nanoparticles. Selective degradation can be devised by using a method of changing the distance between the targeted molecules and the gold nanoparticles.

2. Experimental Section

Chemicals. A commercially available lysozyme (Tokyo Kasei Kogyo Co., Ltd.) and buffer salts employed in the present experiment were used without further purification.

Preparation of Gold Nanoparticles in Pure Water. Gold nanoparticles were produced by laser irradiation of a gold plate in pure water.[20−22] The plate was placed in the bottom of a glass vessel filled with 10 mL of pure water and was irradiated with an output of the fundamental (wavelength of 1064 nm and pulse width of 5 ns) of Quanta-Ray GCR1-170 Nd:YAG laser operating a 10 Hz. The laser beam was focused onto a diameter

* Corresponding author. E-mail: takeda@clusterlab.jp.

10.1021/jp058204v CCC: $33.50
Published on Web 01/19/2006

of ~1 mm on the surface of the metal plate by a lens with a focus length of 250 mm. The average diameter and its standard deviation of the Au nanoparticles were determined to be 13.7 and 2.3 nm, respectively, from the TEM images.

Degradation of Proteins by Laser Irradiation of Gold Nanoparticles. An aqueous solution containing gold nanoparticles (1.3 nM, 14 nm in diameter) and lysozyme was prepared. The pH of the solution was adjusted to 11.0 by adding Tris buffer (10 mM) or to 4.9 by adding ammonium acetate buffer (10 mM). Note that a pH of 11.0 corresponds to the isoelectric point (pI) of lysozyme.[23] Lysozyme molecules in the solution are neutralized and adsorbed on the gold nanoparticles with its pH value adjusted at 11.0. On the other hand, lysozyme molecules are dissolved uniformly with its pH value adjusted at 4.9. These solutions were placed in an optical cell equipped with a stirrer at the bottom. The output of the second harmonic of the Quanta-Ray GCR 170 Nd:YAG laser at the wavelength of 532 nm was focused to a volume of 1 mm^3 in the solution by a lens having a focal length of 250 mm. The wavelength of 532 nm is close to that of the surface plasmon band of Au nanoparticles. An OPHIR 10A-P-AN power meter was used to monitor the laser power. The degree of lysozyme degradation was determined by sodium dodecyl sulfate (SDS)-polyacrylamide gel electrophoresis. The optical absorption spectrum of the solution was measured by a Shimadzu UV-1200 spectrometer. We also carried out control experiments by using solutions without Au nanoparticles.

3. Results

Panels a and b in Figure 1 show pictures of the SDS-polyacrylamide electrophoresis gels obtained from an aqueous solution of lysozyme (3.6 μM) with pH values of 11.0 (Tris buffer (10 mM)) and 4.9 (ammonium acetate buffer (10 mM)), respectively, containing gold nanoparticles (1.3 nM), after the solutions were irradiated with a pulse laser (532 nm, 17 mJ/pulse) for different irradiation times. The arrows in panels a and b indicate the position of lysozyme in the electrophoresis gels. As the laser irradiation time increases, the intensity of the lysozyme band shown in panel a decreases more rapidly than that in panel b. As shown in panel c, the degree of lysozyme degradation increases with the irradiation time. To quantify the degradation of lysozyme, we correlate the degree of lysozyme degradation to the intensity of the lysozyme band; that is, at a time of zero ($t = 0$), the degree of degradation is regarded to be zero while a zero intensity of the lysozyme band corresponds to unity in the degree of degradation. The degree of lysozyme degradation (Deg(t)) can be quantified as

$$\mathrm{Deg}(t) = 1 - I(t)/I(0)$$

where $I(t)$ represents the intensity of the lysozyme band at an irradiation time, t (min), and $I(0)$ is the band intensity at $t = 0$. The solid circles and the solid squares indicate the degree of lysozyme degradation when the pH values of the solutions were set to 11.0 and 4.9, respectively. The solid lines in panel c show the fitting curves by assuming an equation,

$$f(t) = 1 - \exp(-t/\tau) \qquad (1)$$

where $1/\tau$ represents the degradation rate of the lysozyme. The validity of eq 1 is argued in the Discussion section. The $1/\tau$ values at pH values of 11.0 and 4.9 are $(7.2 \pm 0.9) \times 10^{-2}$ s^{-1} and $(1.1 \pm 0.1) \times 10^{-2}$ s^{-1}, respectively. The fitting curves reproduce the dependence of the degree of lysozyme degradation on the irradiation time.

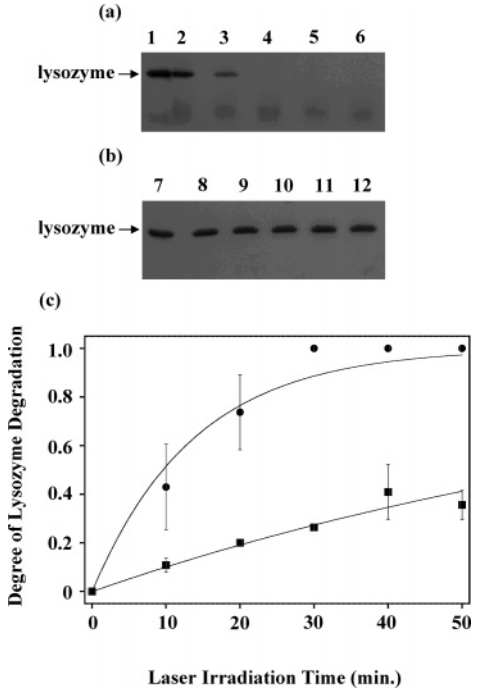

Figure 1. (a and b) SDS-polyacrylamide electrophoresis gels of an aqueous solution of lysozyme dispersed with gold nanoparticles, which were irradiated by intense laser (532 nm, 17 mJ/pulse) for different irradiation times when the pH values of the solution were set to 11.0 (a) and 4.9 (b). The numbers on each picture represent lane numbers for solutions exposed for different irradiation times; lane 1 and 7 are for 0 min, lane 2 and 8 are for 10 min, lane 3 and 9 are for 20 min, lane 4 and 10 are for 30 min, lane 5 and 11 are for 40 min, and lane 6 and 12 are for 50 min. The arrows in the left-hand margins of the lanes in a and b indicate the position of a lysozyme band. (c) Degree of lysozyme degradation plotted against the irradiation time. The solid circles and the solid squares indicate the degree of lysozyme degradation when the pH values of the solution were set to 11.0 and 4.9, respectively. A degree of lysozyme degradation of unity indicates that lysozyme in the solution is fully degraded. The solid lines in c represent the curve fitting to the data by using eq 1.

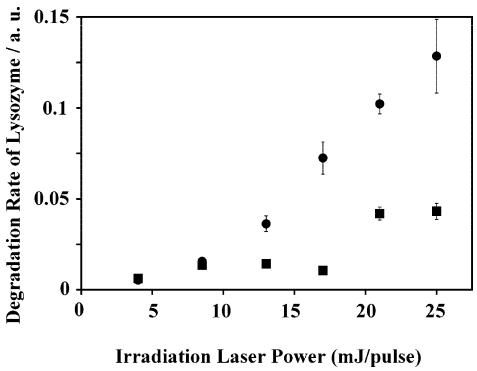

Figure 2. Degradation rate of lysozyme as a function of the laser power. The solid circles and the solid squares indicate the degradation rate of lysozyme when the pH values of the solution are 11.0 and 4.9, respectively.

Figure 2 shows the degradation rate of lysozyme as a function of an irradiation laser power (mJ/pulse). The solid circles and the solid squares indicate the degradation rates of lysozyme for aqueous solutions of lysozyme with pH values of 11.0 and 4.9, respectively. The degradation rate increases with the laser power both at pH = 11.0 and 4.9, although the degradation rate at pH = 11.0 is larger than that at pH = 4.9 at a given laser power in the entire power range studied.

Figure 3 shows the degree of lysozyme degradation plotted against the irradiation time in solutions without Au nanoparticles

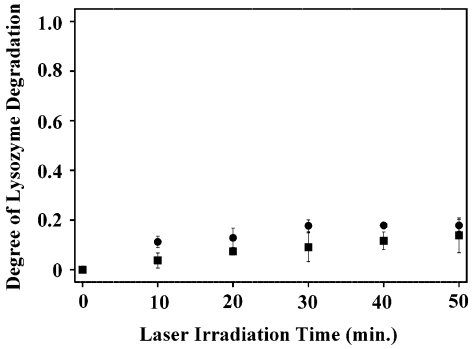

Figure 3. Degree of lysozyme degradation plotted against the irradiation time in solutions without Au nanoparticles as control experiments. The solid circles and the solid squares indicate the degree of lysozyme degradation when the pH values of the solutions were set to 11.0 and 4.9, respectively.

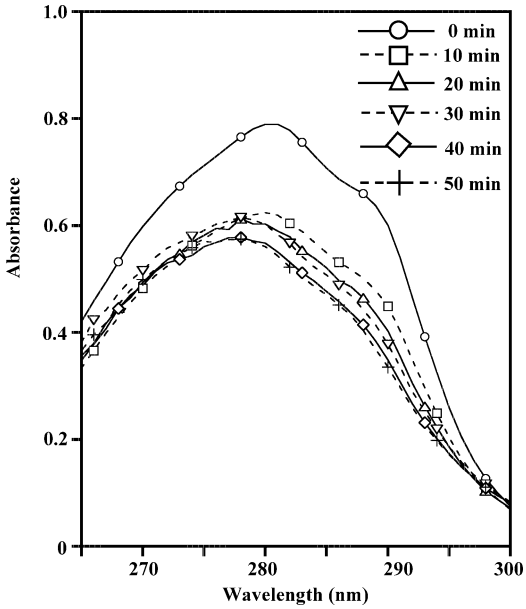

Figure 4. Optical absorption spectra of an aqueous solution of lysozyme containing gold nanoparticles (1.3 nM) for different irradiation times (532 nm, 8.5 mJ/pulse).

as control experiments. The solid circles and the solid squares show the degrees of lysozyme degradation when the pH values of the solution were set to 11.0 and 4.9, respectively. It was revealed that lysozyme degradation by laser irradiation did not occur in the solution without Au nanoparticles.

Figure 4 shows optical absorption spectra of an aqueous solution of lysozyme containing gold nanoparticles with a pH of 11.0 obtained at different irradiation times of a 532-nm laser having a power of 8.5 mJ/pulse so as to identify chemical species produced after the degradation of lysozyme. The absorption band at ~280 nm is ascribed to tryptophan and tyrosine residues in lysozyme, and the band at 290 nm to tryptophan residues.[24] The absorption bands at 290 and 280 nm are weakened increasingly as the laser irradiation time increases.

Figure 5 shows a correlation between the degree of lysozyme degradation and an absorption decrement at 290 nm or that at 280 nm for a given irradiation time. The solid circles and the open squares show absorption decrements at 290 and 280 nm, respectively. In Figure 5, the slope (0.52 ± 0.02) of the linear solid line for the 290-nm data is related to the ratio of the reduction amount of the tryptophan residues in a lysozyme molecule to the degree of lysozyme degradation, and the slope (0.42 ± 0.02) of the linear dotted line for the 280-nm data is

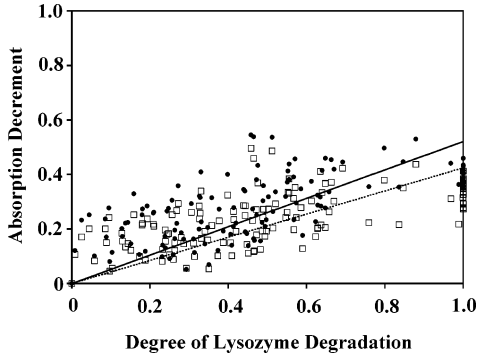

Figure 5. Correlation between the degree of lysozyme degradation and the absorption decrement at 290 nm and that at 280 nm in the optical absorption spectra shown in Figure 4. The solid circles and the open squares correspond to the decrement at 290 and 280 nm, respectively. The solid and dotted lines are curves fitted to the data at 290 and 280 nm, respectively.

related to the ratio of the decrease in the amount of the tryptophan and tyrosine residues in a lysozyme molecule to the degree of lysozyme degradation. Thus, the intensity of the absorption band at 290 nm decreases a little more rapidly than that at 280 nm as the laser irradiation time increases.

4. Discussion

Region of Nanoplasma Formation. Gold nanoparticles undergo resonant multiphoton excitation through the surface plasmon mode much more efficiently than water does under irradiation of a 532-nm laser on an aqueous solution of lysozyme containing gold nanoparticles. The power of the laser which irradiates the solution is set at such a level that multiphoton ionization occurs only in the gold nanoparticles and not in water.[25−27] In reality, this can be realized because the threshold power density for plasma formation in water ($\sim 10^{10}$ W/cm^2)[28] is much higher than the power density ($\sim 10^9$ W/cm^2) of the irradiation laser employed in the present experiment. Under irradiation of a laser having such a power density, seed-electrons are produced exclusively in the laser-excited gold nanoparticle from which plasma is produced; in the plasma, densely populated electrons are kinetically heated in a heated high-pressure water medium.[29−31]

It is estimated that (1) the temperature of a laser-excited gold nanoparticle reaches as high as 10^4-10^5 K as a result of the multiphoton excitation of the gold nanoparticle[21,32,33] and (2) ~0.1% of the constituent gold atoms release electrons since the electron emission efficiency is proportional to $\exp(-W/k_BT)$ with the work function (W) of 5.1 eV for gold metal and the temperature (T) of 10^4-10^5 K. As the number density of gold atoms in a nanoparticle is $\sim 6 \times 10^{22}$ atoms/cm^3, the number density of electrons ejected from the gold nanoparticle by laser irradiation is estimated to be more than $\sim 6 \times 10^{19}$ electrons/cm^3. As shown in a previous study,[34] this number density exceed the critical number density ($\sim 10^{18}$ electrons/cm^3) of electrons required for plasma creation. The threshold power of the laser for formation of nanoplasma was estimated as follows: The critical number density of electrons and the number density of gold atoms in an Au nanoparticle are 10^{18} electrons/cm^3 and 10^{23} atoms/cm^3, respectively. Therefore, the ratio of 1.7×10^{-3} of constituent Au atoms in an Au nanoparticle should be ionized for nanoplasma formation. The thermal electron emission efficiency is proportional to $\exp(-W/k_BT)$. Therefore, the threshold temperature T_{th} of the Au nanoparticles for nanoplasma formation is calculated to be 0.9×10^4 K by resolving the equation $\exp(-W/k_BT_{th}) = 1.7 \times 10^{-3}$. The laser power required

for rising the temperature of Au nanoparticles above the threshold temperature T_{th} is estimated to be 1.3 mJ/mm^2.

The volume of the plasma is estimated on the basis of a theoretical study on plasma formation by laser irradiation in solution. The rate equation for the free electron density (ρ) in the plasma is given as[30,31]

$$\frac{d\rho}{dt} = \eta\rho - g\rho + \left[\frac{d\rho}{dt}\right]_m$$

The first term on the right-hand side represents cascade multiplication of free electrons; the cascade ionization rate (η) is given by a probability per unit time of a free electron undergoing ionizing collision with a bound electron. During one laser pulse, this process continues in a region where seed electrons are present. The second term represents a decrement of the electron density due to recombination, trapping, and diffusion. The rate constant (g) includes all contributions of these processes. The last term represents the generation of seed-electrons in a gold nanoparticle by multiphoton ionization during cascading. It is approximated that the volume of the plasma is mainly determined by the volume in which free electrons (for seeding) ejected from a laser-excited gold nanoparticle are present in the early stage of the laser irradiation; the density of the free seed-electrons depend on the rates of recombination, trapping, and diffusion of the free electrons. Let us assume that the average lifetime of the free seed-electrons is longer than the width of a laser pulse during which the electrons are absorbing energy from the intense optical field.[30,31] It is reported that electron−hole recombination in plasma can be disregarded.[36] The electrons are not trapped for a significantly long time in localized potential wells such as solvated states because the binding energies for the trapping are so low that the electrons are easily detached by electron collision and/or by photon absorption. Under these circumstances, we can safely assume that the trapping and detaching of free seed-electrons do not significantly affect the plasma formation process.

The upper limit of the volume in which seed-electrons are present is, therefore, determined by the diffusion length of the electrons. First, the upper limit of the diffusion length of the seed electrons ejected from a laser-excited gold nanoparticle in the duration of a single laser pulse, $d_{upperlimit}$, is given by the following equation:

$$d_{upperlimit} = \sqrt{D\tau_p} \quad (2)$$

where D is the electron diffusion coefficient, and τ_p is the temporal width of a laser pulse. The electron diffusion coefficient is given by

$$D = 2\epsilon_{av}/3m\nu \quad (3)$$

where ϵ_{av} is the average electron energy, m is the mass of a free electron, and ν is an effective frequency for collision with water molecules. The values of ϵ_{av} and ν are given by

$$\epsilon_{av} = E_{ion}/2 \quad (4)$$

and

$$\nu = 1/\tau_c \quad (5)$$

where E_{ion} is the electron binding energy and τ_c is the collision time for momentum transfer. An electron binding energy, E_{ion}, is as high as the work function of a gold metal (5.1 eV) and τ_c is 1.0×10^{-15} s.[28] The value of D was obtained to be 5.9×10^{-5} m^2/s by using eqs 3−5. The parameter $d_{upper\,limit}$ turns out to be ∼700 nm by substituting D and τ_p into eq 2. The actual volume of the plasma should be much smaller than that estimated from $d_{upper\,limit}$, because of Coulomb interactions between electrons and positively charged gold nanoparticles, the decrease of electron density by electron diffusion, etc., which are disregarded in the above estimation. Moreover, if all the constituent gold atoms in a laser-excited gold nanoparticle emit electrons, the electron density reaches as high as $\sim 6 \times 10^{19}$ electrons/cm^3. A volume in which the electron density is higher than the threshold electron density for plasma formation ($\sim 10^{18}$ electrons/cm^3) is estimated to be $(\sim 10^{-7}\text{m})^3$, if these electrons can diffuse out of the gold nanoparticle. As described above, plasma produced from a laser-excited gold nanoparticle is estimated to be confined in a volume as small as $(\sim 10^{-7}\text{m})^3$. Therefore, we name it "nanoplasma".

Degradation of the Lysozyme by Nanoplasma. Nanoplasma formed around Au nanoparticles simultaneously induces with local heating. It is difficult to investigate whether local heating or other high-energy particles such as electrons and gold ions degrade the lysozyme molecules. However, local heating produced around Au nanoparticles does not lead to degradation of the biomolecules attached to Au nanoparticles.[37] Especially, local heating produced by irradiation of a laser with a power lower than the threshold power of nanoplasma generation does not lead to degradation of the protein adsorbed on Au nanoparticles. It is considered that proteins tend to escape from the surface of Au nanoparticles by local heating because the adsorption energy of the proteins on the Au nanoparticles is substantially lower than the thermal energy attained around Au nanoparticles by laser irradiation.[38] It is naturally concluded, therefore, that high-energy particles rather than local heating produced by the laser irradiation play a major role in degrading the lysozyme. Let us consider degradation of lysozyme under irradiation of a 532-nm laser in an aqueous solution of lysozyme containing gold nanoparitcles. The degradation is found to proceed most efficiently at pH = 11.0, at which lysozyme molecules are neutralized so that almost all of them are adsorbed on the gold nanoparticles.[38] As nanoplasma is produced in the vicinity of a laser-excited gold nanoparticle, it is concluded that lysozyme molecules are degraded in nanoplasma. This scheme is confirmed by the result that no degradation occurs without gold nanoparticles. Assuming that every gold nanoparticle under laser irradiation creates a nanoplasma, the total volume of the nanoplasmas created by all the gold nanoparticles is calculated to be 10^{-3} times as large as the total volume of the solution containing 1.3 nM gold nanoparticles, considering the estimation of the maximum volume of a single nanoplasma, $\sim 10^{-21}$ m^3. Lysozyme molecules are dissolved homogeneously in a solution with a pH of 4.9, and hence, degradation takes place less efficiently since the distribution of lysozyme molecules within the nanoplasma would be much lower.

Gold nanoparticles are fragmented and regenerated repeatedly under irradiation of a laser,[33,34] and otherwise, the degree of lysozyme degradation would be much smaller than that actually observed. Let us consider the situation that gold nanoparticles are fragmented by laser excitation but are not regenerated; in other words, the gold nanoparticles participate in lysozyme degradation only once. If lysozyme molecules are degraded in nanoplasma, the degree of lysozyme degradation in a solution with a pH of 4.9 is given by the ratio of the total volume of nanoplasma in the solution to the volume of the solution, i.e., $\sim 10^{-3}$. The degree of lysozyme degradation thus estimated ($\sim 10^{-3}$) is extremely low compared to that observed. Then, we

reach an inescapable conclusion that gold nanoparticles participate in lysozyme degradation through repeated cycles of photofragmentation and aggregation. Actually, it has been shown that gold nanoparticles are reconstructed by the aggregation of fragmented gold atoms after laser irradiation.[39,40] As shown in Figure 1, the degree of lysozyme degradation is more than 0.36 $\pm$ 0.06 for the irradiation time of 50 min at a pH of 4.9. In the scheme of repetitive laser degradation, the dependence of the degree of lysozyme degradation on the irradiation time is expressed by eq 1.

At a pH of 11.0 (pI of lysozyme), lysozyme molecules are found to be neutralized and aggregated.[23] If the aggregates of lysozyme molecules are dispersed homogeneously in the solution, the degradation rate shall be same as that for the solution with a pH of 4.9. However, the degree of lysozyme degradation at pH = 11.0 is larger than that at pH = 4.9. This finding implies that almost all the lysozyme molecules are aggregated on gold nanoparticles and, hence, degraded more effectively.

The degradation rate of lysozyme increases with the laser power, as shown in Figure 2, both at pH values of 11.0 and 4.9. This finding is consistent with the scheme that as the laser power increases, seed-electrons ejected from a laser-excited gold nanoparticle increase in number and, hence, the resulting nanoplasma is enlarged increasingly. In addition, the irradiated volume, in which the laser power density exceeds the threshold energy density for nanoplasma generation, increases in size with the laser power.

Fragments Produced by Lysozyme Degradation. Lysozyme molecules were fully degraded by laser irradiation in the presence of gold nanoparticles into fragments whose molecular weight was estimated to be much smaller than 5000 by means of SDS-polyacrylamide gel electrophoresis. As described in the Results section and shown in Figure 4, the absorbance for the tryptophan and tyrosine residues (absorption at 280 nm) and that for the tryptophan residue (absorption at 290 nm) decreases with an increase in the degree of lysozyme degradation. These results indicate that lysozyme molecules are degraded into peptide or amino acid fragments and that , to some extent, indole rings of tryptophan and aromatic rings of tyrosine and phenylalanine are ruptured.

The absorption decrement at 290 nm can be used as a propensity measurement showing the degree of rupture of indole rings in a lysozyme molecule, while the absorption decrement at 280 nm can be use as that showing the degree of rupture of indole and aromatic rings. As shown in Figure 5, the decrement in the absorption at 290 nm is 0.52 $\pm$ 0.02 at the degree of lysozyme degradation and that at 280 nm is 0.42 $\pm$ 0.02. These results indicate that the decrement is smaller than the degree of lysozyme degradation. This finding shows that part of the indole and aromatic rings are not degraded in the lysozyme degradation by nanoplasma and they can escape from the surface of the gold nanoparticles so that they are not ruptured by later laser irradiation.

5. Conclusions

We demonstrated lysozyme degradation by nanoplasma created by laser irradiation of gold nanoparticles in an aqueous solution containing lysozyme and gold nanoparticles. The advantage of this method is that (1) the volume of the lysozyme degradation is confined in a small volume of about 10^{-21} m^3 around a laser-excited gold nanoparticle and (2) the lysozyme degradation can be performed in a selective manner by changing the distance between a lysozyme molecule and a gold nanoparticle by controlling the affinity between them. This method is applicable to the degradation of other proteins as well.

Acknowledgment. This research was supported by the Special Cluster Research Project of Genesis Research Institute, Inc.

References and Notes

(1) Sacchi, C. A. *J. Opt. Soc. Am. B* **1991**, *8*, 337.
(2) Yui, H.; Sawada, T. *Phys. Rev. Lett.* **2000**, *85*, 3512.
(3) Yui, H.; Sawada, T. *Rev. Sci. Instrum.* **2003**, *74*, 456.
(4) Noack, J.; Vogel, A. *IEEE J. Quantum Electron.* **1999**, *35*, 1156.
(5) Smith, W. L.; Liu, P.; Bloembergen, N. *Phys. Rev. A* **1977**, *15*, 2396.
(6) Vogel, A.; Nahen, K.; Theisen, D.; Noack J. *IEEE J. Sel. Top. Quantum Electron.* **1996**, *2*, 847.
(7) Nahen, K.; Vogel, A. *IEEE J. Sel. Top. Quantum Electron.* **1996**, *2*, 861.
(8) Hammer, D. X.; Thomas, R. J.; Noojin, G. D.; Rockwell, B. A.; Kennedy, P. K.; Roach W. P. *IEEE J. Quantum Electron.* **1996**, *32*, 670.
(9) Cremers, D. A.; Radziemski, L. J.; Loree, T. R. *Appl. Spectrosc.* **1984**, *38*, 721.
(10) Carranza, J. E.; Hahn, D. W. *Anal. Chem.* **2002**, *74*, 5450.
(11) Radziemski, L. J.; Loree, T. R.; Cremers, D. A.; Hoffman, N. M. *Anal. Chem.* **1983**, *55*, 1246.
(12) Ottesen, D. K.; Wang, J. C. F.; Radziemski, L. J. *Appl. Spectrosc.* **1989**, *43*, 967.
(13) Núñez, M. H.; Cavalli, P.; Petrucci, G.; Omenetto, N. *Appl. Spectrosc.* **2000**, *54*, 1805.
(14) Vogel, A. *Phys. Med. Biol.* **1997**, *42*, 895.
(15) Berns, M. W. *Sci. Am.* **1991**, *264*, 84.
(16) Anderson, R. R.; Parrish, J. A. *Science* **1983**, *220*, 524.
(17) Feng, Q.; Moloney, J. V.; Newell, A. C.; Wright, E. M.; Cook, K.; Kennedy, P. K.; Hammer, D. X.; Rockwell, B. A.; Thompson C. R. *IEEE J. Quantum Electron.* **1997**, *33*, 127.
(18) Esenaliev, R. O.; Karabutov, A. A.; Podymova, N. B.; Letokhov. V. S. *Appl. Phys. B* **1994**, *59*, 73.
(19) Kesavamoorthy, R.; Super, M. S.; Asher S. A. *J. Appl. Phys.* **1992**, *71*, 1116.
(20) Mafuné, F.; Kohno, J.; Takeda, Y.; Kondow, T. Sawabe H. *J. Phys. Chem. B* **2001**, *105*, 5114.
(21) Mafuné, F.; Kohno, J.; Takeda, Y.; Kondow, T. *J. Phys. Chem. B* **2002**, *106*, 7575.
(22) Mafuné, F.; Kohno, J.; Takeda, Y.; Kondow, T. *J. Phys. Chem. B* **2003**, *107*, 12589.
(23) Jansen, E. F.; Tomimatsu, Y.; Olson, A. C. *Arch. Biochem. Biophys.* **1971**, *144*, 394.
(24) Izumi, T.; Inoue, H. *J. Biochem.* **1976**, *79*, 1309.
(25) McGrath, T. E.; Beveridge, A. C.; Diebold, G. J. *Angew. Chem., Int. Ed.* **1999**, *38*, 3353.
(26) Izumida. S.; Onishi, K.; Saito, M. *Jpn. J. Appl. Phys., Part 1* **1998**, *37*, 2039.
(27) Takeda, Y.; Kondow, T.; Mafuné, F. *Nucleosides, Nucleotides Nucleic Acids* **2005**, *24*, 1215.
(28) Kennedy, P. K.; Boppart, S. A.; Hammer, D. X.; Rockwell, B. A.; Noojin, G. D.; Roach, W. P. *IEEE J. Quantum Electron.* **1995**, *31*, 2250.
(29) Lin, C. P.; Kelly, M. W. *Appl. Phys. Lett.* **1998**, *72*, 2800.
(30) Löwen H.; Madden P. A. *J. Chem. Phys.* **1992**, *97*, 8760.
(31) McEwan, K. J.; Madden, P. A. *J. Chem. Phys.* **1992**, *97*, 8748.
(32) Takami, A.; Kurita, H.; Koda, S. *J. Phys. Chem. B* **1999**, *103*, 1226.
(33) Kurita, H.; Takami, A.; Koda, S. *Appl. Phys. Lett.* **1998**, *72*, 789.
(34) Kennedy, P. K. *IEEE J. Quantum Electron.* **1995**, *31*, 2241.
(35) Shen, Y. R. *The Principles of Nonlinear Optics*; Wiley: New York, 1984.
(36) Lenzner, M.; Krüger, J.; Sartania, S.; Chend, Z.; Spielmann, Ch.; Mourou, G.; Kautek, W.; Krausz, F. *Phys. Rev. Lett.* **1998**, *80*, 4076.
(37) Hamad-Schifferli, K.; Schwartz, J. J.; Santos, A. T.; Zhang S.; Jacobson J. M. *Nature* **2002**, *415*, 152.
(38) Huettmann, G.; Radt, B.; Serbin, J.; Birngruber, R. *Proc. SPIE-Int. Soc. Opt. Eng.* **2003**, *5142*, 88.
(39) Mafuné, F.; Kohno, J.; Takeda, Y.; Kondow, T. *J. Phys. Chem. B* **2002**, *106*, 8555.
(40) Mafuné, F.; Kohno, J.; Takeda, Y.; Kondow, T. *J. Phys. Chem. B* **2001**, *105*, 9050.